Original Article

Diffusion kurtosis imaging (DKI) of hepatocellular carcinoma: correlation with microvascular invasion and histologic grade

Likun Cao[1], Jie Chen[1], Ting Duan[1], Min Wang[2], Hanyu Jiang[1], Yi Wei[1], Chunchao Xia[1], Xiaoyue Zhou[3], Xu Yan[3], Bin Song[1]

[1]Department of Radiology, West China Hospital of Sichuan University, Chengdu 610041, China; [2]Department of Radiology, Inner Mongolia People's Hospital, Hohhot 010017, China; [3]Siemens Healthcare Ltd., Shanghai 201318, China

Correspondence to: Bin Song. Department of Radiology, West China Hospital of Sichuan University, No. 37 Guo Xue Xiang, Chengdu 610041, China. Email: songb_radiology@163.com.

Background: The aim of this study was to prospectively evaluate the diagnostic efficacy of diffusion kurtosis imaging (DKI) in predicting microvascular invasion (MVI) and histologic grade of hepatocellular carcinoma (HCC) with comparison to the conventional diffusion-weighted imaging (DWI).

Methods: This prospective study was approved by the Institutional Review Board, and written informed consent was obtained from all patients. From September 2015 to January 2017, 74 consecutive HCC patients were enrolled in this study. Preoperative magnetic resonance imaging including DKI protocol was performed, and patients were followed up for at least one year after surgery. Diffusion parameters including the mean corrected apparent diffusion coefficient (MD), mean apparent kurtosis coefficient (MK), and apparent diffusion coefficient (ADC) were calculated. Differences of diffusion parameters among different histopathological groups were compared. For parameters that were significantly different between pathological groups, receiver operating characteristics (ROC) curve analyses were performed to evaluate the diagnostic efficiency for identifying MVI and predicting high-grade HCC. Univariate and multivariate logistic regression analyses were used to evaluate the relative value of clinical and laboratory variables and diffusion parameters as risk factors for early recurrence (≤1 year).

Results: Among all the studied diffusion parameters, only MK differed significantly between the MVI-positive and MVI-negative group (0.91±0.10 *vs.* 0.82±0.09, P<0.001), and showed moderate diagnostic efficacy (AUC =0.77) for identifying MVI. High-grade HCCs showed significantly higher MK values (0.93±0.10 *vs.* 0.82±0.09, P<0.001), along with MD (1.34±0.18 *vs.* 1.54±0.22, P<0.001) and ADC values (1.17±0.15 *vs.* 1.30±0.16, P=0.001) than low-grade HCCs. For differentiating high-grade from low-grade HCCs, MK demonstrated a higher area under the ROC curve (AUC) and significantly higher specificity than MD and ADC (AUC =0.81 *vs.* 0.76 and 0.74; specificity =82.2% *vs.* 60.0% and 60.0%, P=0.02). In addition, higher MK (OR =5.700, P=0.002) and Barcelona Clinic Liver Cancer (BCLC) stage C (OR =6.329, P=0.005) were independent risk factors for early HCC recurrence.

Conclusions: DKI-derived MK values outperformed conventional ADC values for predicting MVI and histologic grade of HCC, and are associated with increased risk of early tumor recurrence.

Keywords: Hepatocellular carcinoma (HCC); apparent diffusion coefficient (ADC); diffusion kurtosis imaging (DKI); histologic grade; microvascular invasion (MVI)

Submitted Oct 17, 2018. Accepted for publication Feb 25, 2019.
doi: 10.21037/qims.2019.02.14
View this article at: http://dx.doi.org/10.21037/qims.2019.02.14

Introduction

Hepatocellular carcinoma (HCC) is a common malignancy worldwide and the second leading cause of cancer-related death (1). Despite the emergence of several new therapeutic modalities, long-term survival of advanced HCC patients remains poor due to high-recurrence rates (2,3). Many biological factors of HCC are related with the notorious tumor recurrence. Microvascular invasion (MVI) is an important predictive factor for poor prognosis after curative liver resection or transplantation (4-7), because it provides the route for tumor cells to access the portal or systemic circulation. It has been reported that the one-year recurrence rate in MVI-positive patients was significantly higher than that in MVI-negative patients (7). In addition, tumor differentiation is also considered as an important predictive factor for patient prognosis (8,9). High-grade HCCs are usually associated with higher recurrence rates and poorer prognosis in comparison with low-grade HCCs (5,6). Unfortunately, information regarding MVI status and tumor differentiation is not routinely available preoperatively, thus, limiting their clinical utility in decision making. Therefore, preoperative radiologic prediction of these histopathological results can allow optimized management of HCC and help improve long-term survival for patients.

Diffusion-weighted imaging (DWI) has been widely applied to characterize and grade hepatic lesions (10-14). Despite an abundant number of favorable results, the validity of conventional DWI is challenged by the fact that it is based on the assumption of Gaussian water diffusion (15). To elaborate, water diffusion in living tissues is more complicated and often displays substantial non-Gaussian properties due to the presence of microstructures, such as cell membranes and other organelles (16).

Diffusion kurtosis imaging (DKI) is a special DWI model which treats water diffusion as non-Gaussian behavior (17). Compared with traditional DWI, this model has been shown to provide greater sensitivity to tissue microstructural complexity with an extender b-value range (18). It is also considered to be the preferred model in terms of model fit and repeatability (19). Improved tumor characterization and grading using DKI parameters compared with traditional DWI has already been reported in many other solid malignancies (20-23). However, only a few recent studies have investigated its biological significance in liver imaging. A direct correlation between kurtosis derived from DKI and cellularity of HCC was reported in fresh liver explants (24). Wang *et al.* (25) were first to suggest that mean kurtosis was significantly correlated with MVI and could yield better predictive accuracy for MVI than ADC. However, few studies have explored the ability of DKI in assessing the histologic grade of HCC and patient prognosis. In addition, the value of DKI for predicting tumor biological behaviors requires further validation.

Therefore, the purpose of this study is to evaluate the efficacy of DKI-derived parameters in the preoperative evaluation of MVI and the histologic grade in HCC patients, with comparison to the conventional mono-exponential model-based ADC value. Additionally, we also explored the correlation between diffusion parameters and the early recurrence risk of HCC after hepatic resection.

Methods

Patients

This prospective study was approved by the Institutional Review Board and written informed consent was obtained from all patients. From September 2015 to January 2017, patients with suspected primary liver cancer based on clinical history or previous ultrasonography and/or computed tomography were consecutively enrolled and underwent a preoperative MR examination with DKI sequence. The inclusion criteria were as follows: (I) primary liver lesions without prior treatment; (II) patients ≥18 years old; (III) without contraindication for contrast-enhanced MRI examinations such as metallic implants, pregnancy or renal insufficiency.

One hundred and fifty-four patients were initially scanned during the study period. Among these patients, 80 were excluded for the following reasons: (I) not eligible for tumor resection or did not receive surgery in our hospital (n=40); (II) lesions histopathologically diagnosed as malignancies other than HCC (n=14); (III) HCCs less than 1 cm in diameter (n=4) or with left sub-phrenic locations (n=10); (IV) poor DWI quality due to respiratory or motion artifacts (n=3); (V) loss to follow-up within one year (n=9). Seventy-four patients were finally included, and the median time interval between MR examination and surgical resection was 4 days (range, 1–8 days).

MRI protocol

All patients were examined using a 3T MR scanner (MAGNETOM Skyra, Siemens Healthcare, Erlangen,

Germany) with an 18-channel phased-array body coil and an integrated spine coil with 12 channels. Patients were asked to fast for 6–8 hours before MR examination. Routine MR imaging sequences included in the standardized scanning protocol were high-spatial-resolution transverse T2-weighted imaging (TR/TE =2,160/100; FOV =433×433 mm^2; matrix size =320×288; slice thickness =6 mm; flip angle =160°), coronal T2-weighted imaging (TR/TE =1,000/96; FOV =400×400 mm^2; matrix size =320×320; slice thickness =3 mm; flip angle =160°), T1-weighted in- and opposed-phase imaging (TR/TE =81/1.4; FOV =400×325 mm^2; matrix size =352×286; slice thickness =6 mm; flip angle =70°). For the dynamic phase imaging, Gd-EOB-DTPA (Primovist®; Bayer Schering Pharma AG, Berlin, Germany) was injected intravenously at a dose of 0.025 mmol/kg, followed by a 30-mL bolus of saline. Pre-contrast, late arterial phase (30–40 s), portal venous phase (60–70 s), transitional phase (3 min) and hepatobiliary phase (20 min) were obtained using fat-suppressed axial T1-weighted three-dimensional volume interpolated breath-hold examination (VIBE) sequence (TR/TE =3.95/1.92; FOV =400×295.6 mm^2; matrix size =352×256; slice thickness =2 mm; flip angle =9°).

DKI data was acquired before the administration of contrast agent using a single-shot echo-planar (SS-EPI) diffusion sequence under free breathing. Five b-values (0, 200, 700, 1,400, and 2,100 s/mm^2) in three orthogonal directions were used and the number of averages for each b-value was 1, 1, 2, 4 and 6, respectively. Parallel imaging was used to shorten the scan time and reduce image distortion, with the scanning parameters being the following: TR/TE =5,600/63 ms; FOV =380×289 mm^2; matrix size =100×76; slice thickness =6 mm with a slice gap of 1 mm; voxel size =3.8×3.8×6 mm^3; flip angle =90°, and the total acquisition time =3 minutes and 53 seconds.

Image analysis

Post-processing of diffusion data was performed with an in-house developed DKI tool using a computing language and interactive environment (MATLAB; Mathworks, Natick, MA, USA) (21) to obtain both the DKI parameters and ADC values. A Gaussian filter was first applied in the software with a full width at a half maximum of 3 mm to suppress diffusion imaging noise data. Then, the corrected apparent diffusion coefficient (D) and the apparent kurtosis coefficient (K) were calculated from the multi-b diffusion data using a voxel-by-voxel analysis based on the following formula:

$$S(b)/S(0) = \exp(-b\times D + b^2\times D^2\times K/6) \quad [1]$$

S is the signal intensity at a given b-factor, S0 represents the signal without diffusion weighting, D represents the corrected apparent diffusion coefficient (ADC) accounting for non-Gaussian diffusion behavior, and K represents the apparent kurtosis coefficient which signifies the deviation of tissue diffusion from a Gaussian model. According to the above formula, the DKI Tool calculated the mean diffusion coefficient (MD) map and the mean kurtosis coefficient (MK) map from the trace-weighted diffusion signal of three gradient directions. An additional ADC map was reconstructed using the following standard mono-exponential fit with b-values of 0 and 700 s/mm^2:

$$S(b)/S(0) = \exp(-b\times ADC) \quad [2].$$

All quantitative measurements were conducted separately by two independent radiologists (with 15 and 3 years' experiences, respectively) who were blinded to clinical and pathological results. A single representative ROI was drawn carefully along the entire margin of the tumor on the slice where tumors showed their largest transverse diameter on the ADC maps, excluding areas of necrosis and hemorrhage by referring to T2-weighted and contrast-enhanced T1-weighted images. The ROI was then automatically, simultaneously and unchangeably copied to both MD and MK maps by the aforementioned post-processing software. ADC, MD and MK values were calculated within the same ROI. In patients with multifocal lesions, the largest lesion was chosen as the study target. The parametric values of the ROIs from two measurers were averaged for the final analysis.

Histopathological analysis

Histopathological examination was performed for all the surgically resected hepatic specimens. The presence or absence of MVI and histologic differentiation grade of HCC were blindly identified and used for radiologic-pathologic correlation. MVI was defined as a tumor within a vascular space lined by endothelium that was visible only on microscopy (26). The major histological grade of HCC (the predominant grade within tumor) was determined according to the Edmondson-Steiner classification (27). Tumors with Edmondson-Steiner grade I and II were classified into the low-grade group, and grade III and IV were classified into the high-grade group.

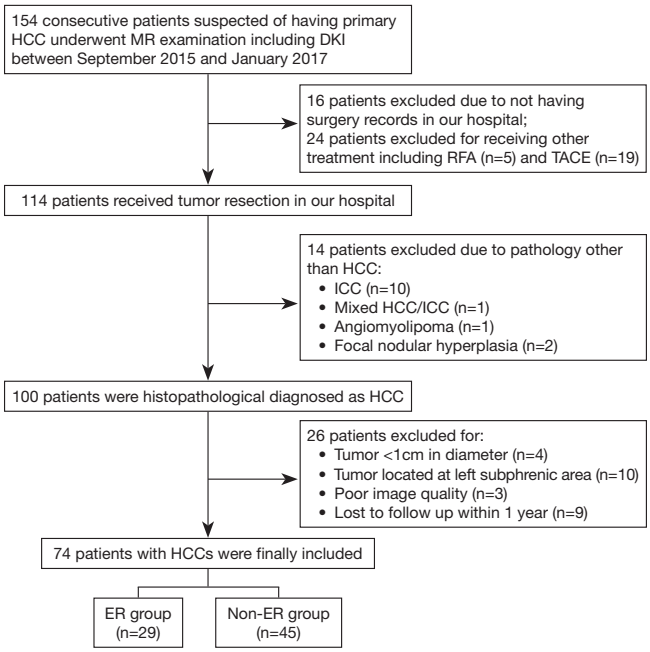

Figure 1 Flowchart shows process of enrollment of study population for this prospective study. ER, early recurrence; HCC, hepatocellular carcinoma; ICC, intrahepatic cholangiocarcinoma; RFA, radiofrequency ablation; TACE, transcatheter arterial chemoembolization.

Follow-up

After surgical resection, all patients were followed up for at least 12 months. The diagnosis of tumor recurrence and metastasis was based on regular image examinations with ultrasonography and/or contrast-enhanced CT, supplemented with X-ray, bone scan and serum AFP elevation. Gadoxetic-acid-enhanced MRI or positron emission tomography were obtained when US and CT failed to provide obvious evidence for a suspected recurrence.

Early recurrence of HCC was identified as the presence of new intrahepatic lesions with typical radiologic features of HCC on two radiological studies or extrahepatic metastasis within 12 months of initial surgery.

Statistical analysis

Quantitative variables were expressed as mean ± standard deviation (SD). The intra-class correlation coefficient (ICC) was firstly calculated to assess the agreement of quantitative measurement for all diffusion parameters between two independent radiologists and defined as follows: less than 0.5, poor reliability; between 0.5 and 0.75, moderate reliability; between 0.75 and 0.9, good reliability; greater than 0.90, excellent reliability. Independent-sample *t* test or Mann-Whitney U test was used to compare the differences in ADC, MD, and MK values between the MVI-positive and MVI-negative group. One-way ANOVA or Kruskal-Wallis rank test was used to compare the differences of these parameters across four histologic grades. Spearman's correlation analysis was performed to determine the relationship between diffusion parameters and histologic grades. Receiver operating characteristic (ROC) analyses were performed to evaluate the diagnostic performance of significant parameters in predicting the presence of MVI and high-grade HCC. The optimal cut-off point which demonstrated the greatest Youden index and the corresponding sensitivity, specificity, positive and negative likelihood ratio was calculated. Z test was used to compare AUCs. P values <0.05 were considered statistically significant.

Univariate and multivariate binary logistic regression analyses were used to identify independent risk factors of early HCC recurrence. The diffusion parameters were divided into two groups according to the optimal cutoff points on the ROC curves. Significant variables in univariate analysis were included in multivariate stepwise logistic analysis. Odds ratios (OR) and 95% confidence intervals (CIs) were calculated. All data analysis was conducted using SPSS 24.0 (SPSS, Chicago, IL, USA).

Results

Demographic and clinical-pathologic characteristics

A total of 74 patients (mean age, 49.2±10.8 years; range, 26–71 years), including 62 men (mean age, 49.2±10.4 years, range, 26–71 years) and 12 women (mean age, 49.0±13.5 range, 30–65 years), were included for final analysis (*Figure 1*). Early recurrence was found in 29 (39.2%) patients, of which 25 (86.2%) were intrahepatic, 2 (6.9%) were extrahepatic (one with lung metastasis, and one with adrenal metastasis), and 2 (6.9%) were combined intra- and extra-hepatic recurrence. Detailed patient characteristics are summarized in *Table 1*.

DKI parameters and ADC in evaluating MVI

Among all diffusion parameters, only MK values correlated

Table 1 Patients' baseline characteristics of clinical and pathologic findings

Characteristics	Values
Clinical information	
Age (years)†	49.2±10.8 (range, 26–71)
Male/female	62/12
Etiology of liver disease	
Hepatitis B virus	66 (89.2)
Hepatitis C virus	3 (4.1)
Both hepatitis B & C virus	1 (1.4)
Cryptogenic disease	4 (5.4)
Tumor size (cm)†	5.80±2.68 (range, 1.50–10.76)
AFP level (ng/mL)‡	97.4 (range, 1.4–15,824.0)
Serum AST (≥35 IU/L)	40 (54.1)
Serum ALT (≥40 IU/L)	30 (40.5)
Cirrhosis	35 (47.3)
BCLC stage	
0	1 (1.4)
A	14 (18.9)
B	43 (58.1)
C	16 (21.6)
Pathologic findings	
Edmondson-Steiner grade	
Grade I	11 (14.9)
Grade II	34 (45.9)
Grade III	21 (28.4)
Grade IV	8 (10.8)
MVI status	
MVI negative	36 (48.6)
MVI positive	38 (51.4)
Patients with early recurrence (≤1 year)	29 (39.2)

Unless indicated otherwise, data represent the number of patients, with percentages in parentheses. †, data are expressed as mean ± standard deviation with ranges in parentheses. ‡, data are expressed as medians with ranges in parentheses. AFP, alpha-fetoprotein; ALT, alanine aminotransferase; AST, aspartate aminotransaminase; BCLC stage: Barcelona Clinic Liver Cancer stage; MVI, microvascular invasion.

significantly with the presence of MVI. The MK values of MVI-negative HCCs were significantly lower than those of MVI-positive HCCs (*Table 2*, *Figure 2*). For identifying the presence of MVI, MK values demonstrated an AUC of 0.77 (95% CI, 0.66–0.86) with a sensitivity of 68.4% (95% CI, 51.3–82.5%) and a specificity of 75.0% (95% CI, 57.8–87.9%) using a cutoff of 0.86 (*Table 3*, *Figure 3*). No significant differences of MD or the reconstructed ADC values existed between HCCs with and without MVI (*Table 2*).

Figures 4 and *5* show MR images of representative HCCs. The inter-observer agreements of the diffusion parameters between the two radiologists were excellent for both ADC (0.90, 95% CI, 0.85–0.94) and MK (0.93, 95% CI, 0.89–0.95), and good for MD (0.88, 95% CI, 0.83–0.93).

DKI parameters and ADC in the differentiation of the histologic grade

There was a good relationship between the Edmondson-Steiner grades and the MK values (rho =0.570), as well as the MD values (rho =–0.501, P<0.01 for both). A fair relationship was found between the ADC values and the histologic grades (rho =–0.493, P<0.01) (*Table 2*). The ADC, MD, and MK values in the different pathological groups are shown in *Figure 2* and *Table 2*. For discriminating low-grade from high-grade HCCs, MK demonstrated the highest area under the curve (AUC) with a value of 0.81 (95% CI, 0.70–0.89), followed by MD and ADC with the value of 0.76 (95% CI, 0.65–0.85) and 0.74 (95% CI, 0.63–0.84), respectively. No statistically significant differences were observed when comparing the above AUCs. In addition, ROC analysis showed that MK (82.2%) had a significantly higher specificity than that of MD (60.0%, P=0.02) and ADC (60.0%, P=0.02), whereas no significant differences were observed in sensitivity for all parameters (72.4% for MK, 86.2% for MD and 75.9% for ADC, respectively) (*Table 3*, *Figure 6*).

Preoperative predictors of early recurrence

Univariate analysis identified the serum AFP level, Barcelona Clinic Liver Cancer (BCLC) stage C, MD, and MK as independent predictors for early recurrence (P<0.05 for all, *Table 4*). At multivariate analysis, only the increased MK value [OR: 5.700 (95% CI, 1.849–17.578), P=0.002] and the BCLC stage C [OR: 6.329 (95% CI, 1.732–23.121), P=0.005] were identified as independent predictors of early tumor recurrence (*Table 4*).

Table 2 Correlations and comparisons of DKI-derived parameters and apparent diffusion coefficient between different histopathological groups

Parameters	MVI status†			Edmondson-Steiner grades†			
	MVI negative‡ (N=36)	MVI positive (N=38)	P	Low-grade (N=45)	High-grade (N=29)	P	Spearman's correlation
ADC† ($\times10^{-3}$ mm^2/s)	1.29±0.17	1.22±0.16	0.071	1.30±0.16	1.17±0.15	0.001**	–0.493**
MD† ($\times10^{-3}$ mm^2/s)	1.51±0.22	1.41±0.22	0.055	1.54±0.22	1.34±0.18	<0.001**	–0.501**
MK‡	0.82±0.09	0.91±0.10	<0.001**	0.82±0.09	0.93±0.10	<0.001**	0.570**

†, independent-sample t test; ‡, Mann-Whitney U test. **, P value <0.01. ADC, apparent diffusion coefficient; MD, mean corrected apparent diffusion coefficient; MK, mean apparent kurtosis coefficient; MVI, microvascular invasion.

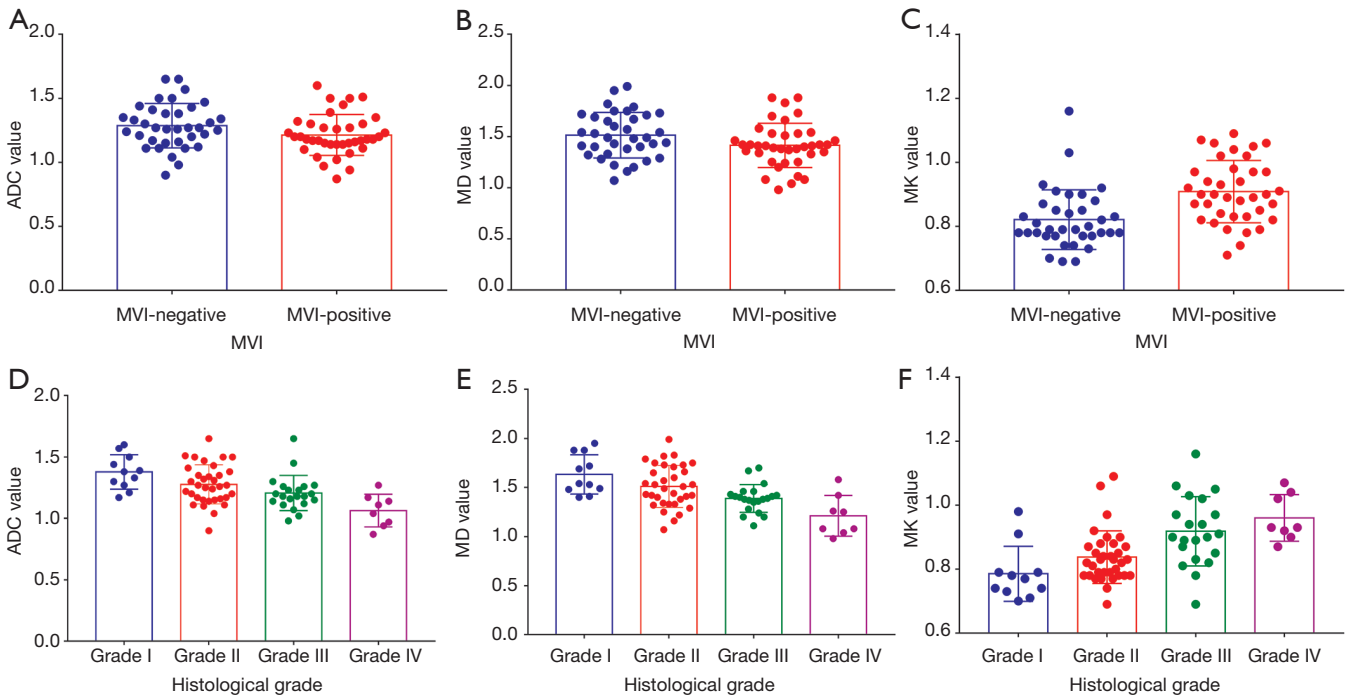

Figure 2 Box and whisker plots represent the differences of the ADC, MD and MK values among different histopathological groups. (A,B,C) Quantitative comparison of the differences between MVI-positive and MVI-negative groups in the ADC, MD, and MK values, respectively. (D,E,F) Quantitative comparison of the differences among four Edmondson-Steiner groups in the ADC, MD, and MK values, respectively. ADC, apparent diffusion coefficient; MD, mean corrected apparent diffusion coefficient; MK, mean diffusion kurtosis coefficient; MVI, microvascular invasion.

Discussion

In this study, we explored the performance of DKI in predicting the presence of MVI and histologic grade of HCC and compared it with the conventional ADC value. Results of this study suggested that among all studied diffusion parameters, MK might be the most promising factor in systematic evaluation of tumor biological behaviors, and serve as an independent risk factor of early recurrence after hepatic resection within a year.

In the present study, encouraging results were observed for the unique DKI-derived parameter—MK. According to the ROC analysis, MK values performed significantly better in predicting both the histological grade and the presence of MVI in HCCs compared with MD and ADC. Although no significant differences were observed in the AUCs, specificity for prediction of high-grade HCCs at the identified threshold was significantly higher for MK

Table 3 Diagnostic value of DKI-derived parameters and ADC value in identifying MVI and differentiating the low-grade group (grade I and II) from the high-grade group (grade III and IV)

Group	AUC (95% CI)	Optimal cutoff value	Sensitivity	Specificity	+LR	−LR
Non-MVI group *vs.* MVI group						
MK	0.77 (0.66–0.86)	≥0.86	68.4% (51.3–82.5%)	75.0% (57.8–87.9%)	2.74	0.42
Low-grade HCC *vs.* high-grade HCC						
ADC	0.74 (0.63–0.84)	≤1.25	75.9% (56.5–89.7%)	60.0% (44.3–74.3%)	1.90	0.40
MD	0.76 (0.65–0.85)	≤1.46	86.2% (68.3–96.1%)	60.0% (44.3–74.3%)	2.16	0.23
MK	0.81 (0.70–0.89)	≥0.89	72.4% (52.8–87.3%)	82.2% (67.9–92.0%)	4.07	0.34

ADC, apparent diffusion coefficient; CI, confidence interval; LR, likelihood ratio; MD, mean corrected apparent diffusion coefficient; MK, mean apparent kurtosis coefficient; DKI, diffusion kurtosis imaging.

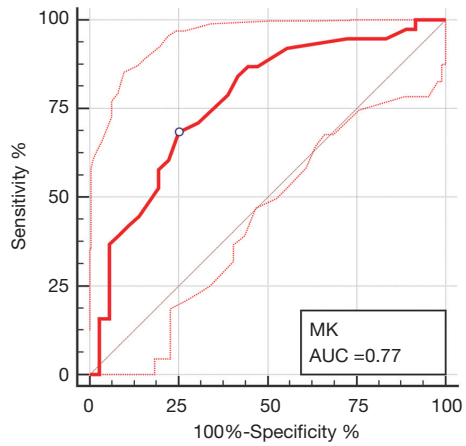

Figure 3 Receiver operating characteristic curve of MK value derived from DKI for identifying MVI. Area under the receiver operating characteristic curve (AUC) for identifying MVI is 0.77, with a cutoff of 0.86. The dashed lines represented the 95% confidence bounds of AUC. MK, mean apparent kurtosis coefficient; MVI, microvascular invasion; DKI, diffusion kurtosis imaging.

than for MD and ADC. Similar results were reported by published studies applying DKI in liver imaging. Goshima *et al.* (28) compared DKI with DWI for assessing therapeutic effects in HCC treatment and observed that MK provided higher diagnostic performance than ADC in evaluating HCC viability. Wang *et al.* (25) were first to report the correlation between DKI and the MVI of HCC. According to them, mean kurtosis value and irregular circumferential enhancement were independent risk factors for the MVI of HCC in multivariate analysis. In addition, they also provided the reason why the DKI-derived MK could yield increased performance in predicting the presence of MVI compared with the conventional ADC value. Firstly, with presence of multiple tissue types such as necrosis, inflammation, tortuous vessels with different permeability, and densely packed cell structures which reflect various distribution of tissue diffusivities, kurtosis is thought to increase in this more complex and heterogenous microenvironment introduced by MVI (15,23). On the other hand, the presence of MVI provide routes for tumor cells to spread to surrounding liver parenchyma (4,7). The vigorous cell proliferation further changes anatomic structure and causes necrosis or hemorrhage, resulting in the increasing tissue complexity at the microstructural level. Finally, these authors also suggest that in MVI-positive HCC, the presence of tumor emboli or clusters of tumor cells in branches of the portal vein, hepatic vein, or capsular vessel could result in the marked hindrance of water motion and interaction with cell membranes, contributing to higher tissue complexity (23). Similar mechanisms can explain the results in this study for tumor differentiation. Because high-grade HCCs tend to be more proliferative, aggressive and heterogeneous, the increased cellularity, tumor cell nuclear-cytoplasmic ratios, and more tortuous extracellular space in high-grade HCCs can result in a more irregular tumor microstructure, similar to MVI (16,17). Therefore, MK is potentially the most specific parameter to reflect tumor biological behaviors. The result that MK was identified as the only significant prognostic factor in both univariate and multivariate analysis in this study could be attributed to the underlying correlation between MK and tumor aggressive biological behaviors.

Meanwhile, ADC and MD values were significantly correlated with the Edmondson-Steiner grade of HCC in this study, which was in consistent with the results of earlier studies and the pooled meta-analysis (29-31). The rationale

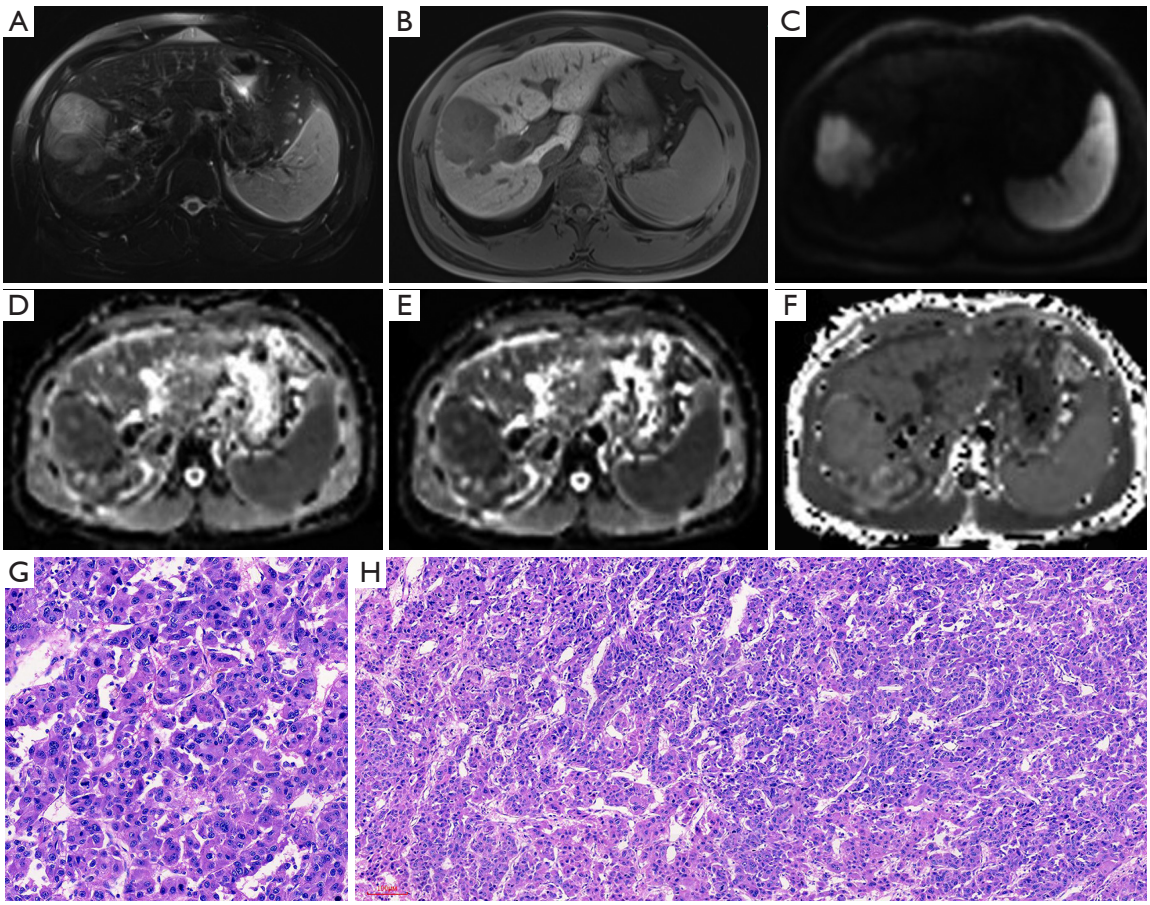

Figure 4 MR images of a 31-year-old male patient with a pathologically verified HCC of Edmondson-Steiner grade III and MVI positive. The patient suffered intrahepatic recurrence at 8 months after tumor resection. A 6.3 cm tumor in right lobe of the liver shows hyperintensity on T2-weighted image (A), hypointensity on 20-min hepatobiliary phase (B) and restricted diffusion on the diffusion-weighted image with a b-value of 700 s/mm^2 (C). ADC (D) and MD maps (E) shows lower signal intensity compared with that of liver parenchyma. MK map (F) shows higher signal intensity of tumor compared with that of background liver parenchyma. The calculated mean values of ADC, MD and MK for the HCC were 1.18×10^{-3} mm^2/s, 1.24×10^{-3} mm^2/s, and 0.96, respectively. The tumor was histopathologically proven to be Edmondson-Steiner III grade with hematoxylin-eosin (HE) staining at 200× magnification (G). The HE staining at 100× magnification (H) showed that increased cellularity, marked variation of nuclear pleomorphism and disorganized distribution of tumor cells with different differentiation degrees. HCC, hepatocellular carcinoma; MVI, microvascular invasion; ADC, apparent diffusion coefficient; MD, mean corrected apparent diffusion coefficient; MK, mean diffusion kurtosis coefficient.

behind this could be that as tumor cellularity increases with the histological grade, this results in the higher density of hydrophobic cellular membranes and decreased extracellular space which subsequently restrict water molecular diffusion and is visually presented as decreased ADC and MD. Based on this, previous studies also attempted to predict the presence of MVI in HCCs using ADC, but their results were controversial. A prior study reported that ADC calculated from b=0 and 500 s/mm^2 images could serve as an independent predictor of MVI in HCC (32). Other studies also reported similar results, suggesting the usefulness of ADC for predicting MVI (33,34). However, the underlying reason behind this is unclear and not confirmed by histopathological analysis so far. The authors (32-34) proposed that possible mechanisms might be that ADC values could reflect capillary perfusion as well as molecular diffusion. Because HCCs with MVI may have decreased perfusion, it would lead to relatively lower ADC

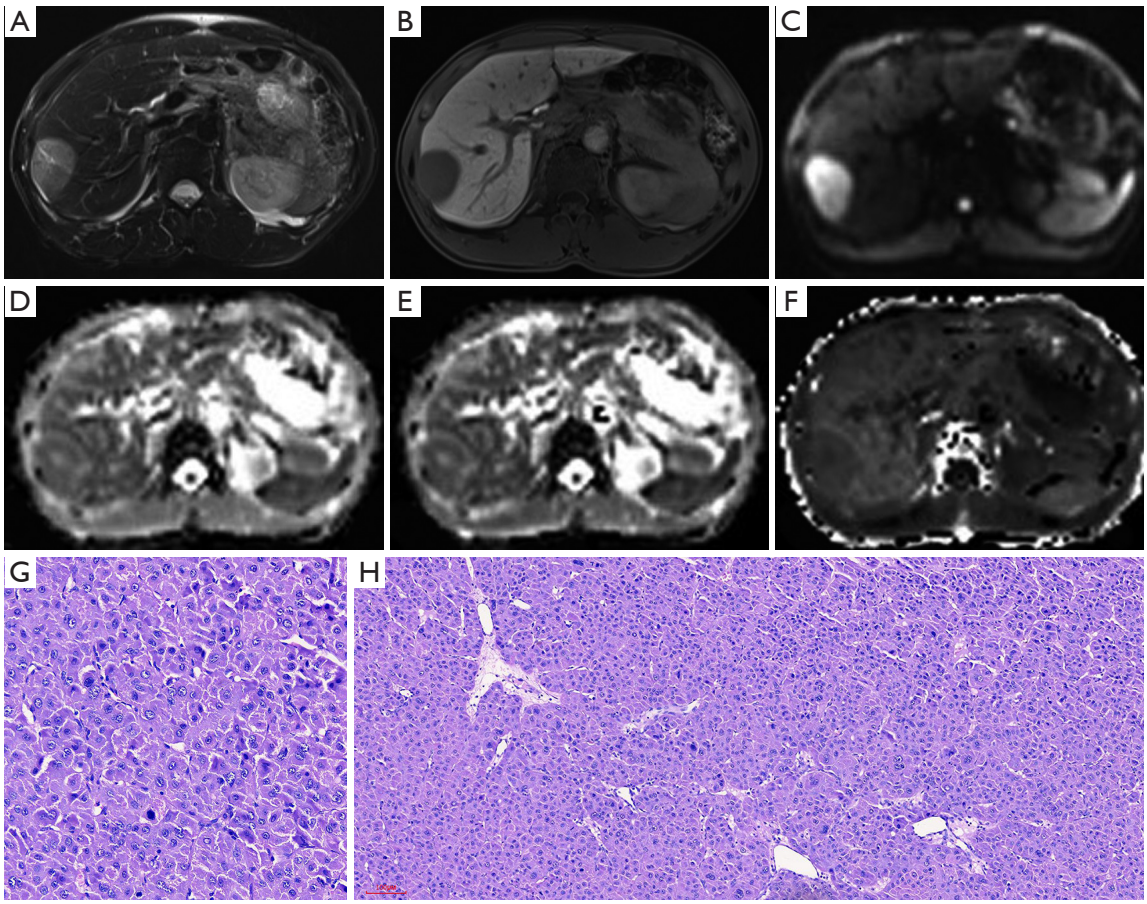

Figure 5 MR images of a 48-year-old male patient with a pathologically verified HCC of Edmondson-Steiner grade II and MVI negative. The patient did not have tumor recurrence within 1 year. A 4.6 cm tumor in the right anterior hepatic section shows hyperintensity on T2-weighted imaging (A), hypointensity relative to the surrounding liver parenchyma in hepatobiliary phase (B), and restrict diffusion on the diffusion-weighted image with a b-value of 700 s/mm^2 (C). ADC (D) and MD maps (E) show slightly higher signal intensity compared with that of liver parenchyma. MK map (F) shows lower slightly lower signal intensity of tumor compared with that of background liver parenchyma. The calculated mean values of ADC, MD, and MK for the HCC were 1.34×10^{-3} mm^2/s, 1.60×10^{-3} mm^2/s and 0.80, respectively. The hematoxylin-eosin (HE) staining of the tumor at 200 × magnification proved it to be Edmonson-Steiner grade II (G). The HE staining at 100× magnification (H) showed that increased cellularity relatively lowered structural complexity. HCC, hepatocellular carcinoma; MVI, microvascular invasion; ADC, apparent diffusion coefficient; MD, mean corrected apparent diffusion coefficient; MK, mean diffusion kurtosis coefficient.

values. In our study, neither ADC nor MD was significantly correlated with the presence of MVI, which was consistent with the results of Li's study (35). This discrepancy, we speculate, is likely to be attributed to the selection of b-values. With high b-values in our study, the influence of microcapillary perfusion on ADC values might be reduced. In addition, because MVI is usually found in venous vessels, the perfusion changes caused by MVI is probably limited, as the relative blood flow velocity is lower in hepatic venous vessels than in arteries. Moreover, the presence of MVI may increase the vascular permeability and reduce the portal vein resistance, causing increased perfusion. Therefore, the aforementioned possible mechanism and the association between ADC, MD, and MVI require further investigation.

It is worth noting that, for the assessment of both tumor histological grade and MVI, similar results were observed for MD and ADC. This finding, to some extent, was in accordance with those of Budjan *et al.* (36) which stated

that the assessment of conventional ADC values could lead to similar results in differentiating liver lesions when using b-values below 1,000 s/mm^2 for MD calculation. This might be explained in terms of their similar physical meanings. Despite the MD value demonstrated potential in reflecting the non-Gaussian diffusion behavior of molecular water in tissue with more precision, it also can be influenced by the "pseudo-diffusion effect" caused by microcirculation of the tissue capillaries like ADC (17,37). Thus, we believe that DKI can provide similar information as traditional DWI does, along with additional information regarding molecule interaction through MK.

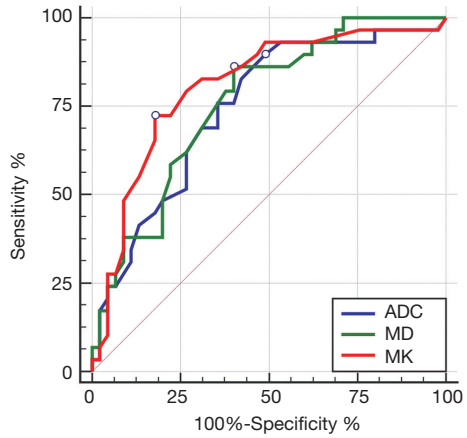

Figure 6 Comparison of ROC curve analysis of DKI-derived parameters and ADC value of hepatocellular carcinoma for differentiating the low-grade HCC from the high-grade HCC. Graph shows that the AUC was largest for MK (AUC =0.81), followed by MD and ADC (AUC =0.76 and 0.74, respectively). There were no significant differences between the AUCs of each parameter. ADC, apparent diffusion coefficient; MD, mean corrected apparent diffusion coefficient; MK, mean apparent kurtosis coefficient; ROC, the receiver operating characteristics; AUC, area under the ROC curve.

Our study also showed that the BCLC stage C was an independent risk factor of early recurrence, which is consistent with the results of previous studies (38,39). ADC was not recognized as a significant predictor in both univariate and multivariate analysis, as with previous studies (13,40). However, Lee *et al.* (41) reported that the mean ADC value was able to predict early recurrence within 2 years in patients with early-stage HCCs (≤5 cm). Other potential risk factors such as age, tumor size, serum AFP levels and cirrhosis were also reported with inconsistent results. The discrepancy may be attributed to the heterogeneity of patient populations evaluated, and the different cut-off points of tumor markers used in the other studies.

Technical parameters and extender b-values setting, which can affect the accurate quantitation of diffusion parameters, are crucial for the DKI model. However, no consensus on this topic has been reached so far, and the best cut-off diffusion values for predicting histopathological

Table 4 Univariate and multivariate analysis in preoperative prediction of one-year early recurrence after hepatectomy in HCC patients

Variable	Univariate analysis		Multivariate analysis	
	OR (95% CI)	P value	OR (95% CI)	P value
Age (y) (≤50/>50)	1.025 (0.403–2.608)	0.959	–	–
AFP (ng/mL) (≤200/>200)	2.966 (1.128–7.801)	0.028*	–	–
BCLC stage				
B stage	1.375 (0.370–5.106)	0.634	–	–
C stage	5.042 (1.101–22.967)	0.037*	6.329 (1.732–23.121)	0.005*
Tumor size (cm) (≤5/>5)	1.309 (0.505–3.395)	0.580	–	–
Cirrhosis	1.339 (0.525–3.415)	0.541	–	–
ADC values (×10^{-3} mm^2/s) (≤1.25/>1.25)	2.171 (0.828–5.694)	0.11	–	–
MD values (×10^{-3} mm^2/s) (≤1.46/>1.46)	3.000 (1.100–8.180)	0.032*	–	–
MK values (≥0.89/<0.89)	3.896 (1.446–10.498)	0.007*	5.700 (1.849–17.578)	0.002*

*, statistically significant results from logistic regression analysis. ADC, apparent diffusion coefficient; AFP, alpha-fetoprotein; BCLC stage: Barcelona Clinic Liver Cancer stage; CI, confidence interval; MD, mean corrected apparent diffusion coefficient; MK, mean apparent kurtosis coefficient; OR, odds ratio.

results may differ greatly between facilities. In most prior studies concerning the usefulness of DKI for breast (21), rectal (42,43) and prostate lesions (22), the b-value spectrum was 0–2,000 s/mm^2. To capture the non-Gaussian distribution behavior of molecular motion, at least two b-values both above and below 1,000 s/mm^2 are usually required (18), with the minimal b-value to mitigate the effect of capillary perfusion on diffusion metrics, and the maximal b-value of approximately 2,000 s/mm^2 to reduce the apparent departure form linearity of the diffusion kurtosis. Merisaari *et al.* (44) suggested that the parameters of the DKI model were best estimated using 5–7 b-values in the range of 300–2,000 s/mm^2. The scan time should also be taken into consideration in routine clinical practice. Accordingly, b-values of 0, 200, 700, 1,400, and 2,100 s/mm^2 were adopted in our study. This DKI protocol yield an overall satisfactory imaging quality and good to excellent inter-observer agreement in our study, suggesting the feasibility of using this DKI model in liver imaging.

Our study had several limitations. First, this is a single-center study with relatively small samples, which enrolled only cases with tumor resection. Thus, it is prone to potential selection bias. Second, predominantly large lesions which tended to be high-grade and MVI positive were enrolled in our study. Third, tumors in the left sub-phrenic area were not included in our study due to the fact that cardiac motion significantly degrades image quality in these areas, causing unreliable measurements; therefore, the results cannot be generalized to left sub-phrenic tumors. Fourth, this DKI protocol was acquired under free-breathing, resulting in decreased signal-to-noise ratio on parameter maps. However, the free-breathing protocol was recommended in several studies (45,46) because of its good reproducibility and shorter acquisition time compared with that of respiratory-triggered and breath-hold imaging. Fifth, the ADC, MD and MK cutoffs were derived from our own population and not tested in a separate validation set, which may have led to an overestimation of performance. Further studies with larger populations in a multicenter setting using standardized DKI protocol should be established to validate our conclusions. Sixth, morphologic imaging findings which were considered to be associated with MVI and early recurrence in many studies were not included into our research for analysis. In future study, HCC-related preoperative clinical information, laboratory data, morphologic imaging findings, and diffusion parameters should be included into multifactorial analysis to select independent risk factors for poor prognosis.

In conclusion, our preliminary study showed that MK values derived from DKI model demonstrated superior diagnostic performance than the conventional ADC value for predicting MVI and poor differentiation of HCC. Higher MK value is associated with more aggressive tumor biological behaviors and increased risk of tumor recurrence.

Acknowledgements

Funding: This study was funded by National Natural Science Foundation of China (Grants NFSC 81471658) and Science and Technology Support Program of Sichuan Province (Grant Number 2017SZ0003, and number 2018SZ0185). The MRI technique in this research was supported by Siemens Healthcare, MR collaboration Northeast Asia.

Footnote

Conflicts of Interest: X Zhou and X Yan are employees of Siemens. The other authors have no conflicts of interest to declare.

Ethical Statement: This prospective study was approved by the Institutional Review Board and written informed consent was obtained from all patients.

References

1. Siegel RL, Miller KD, Jemal A. Cancer statistics, 2018. CA Cancer J Clin 2018;68:7-30.
2. Njei B, Rotman Y, Ditah I, Lim JK. Emerging trends in hepatocellular carcinoma incidence and mortality. Hepatology 2015;61:191-9.
3. Portolani N, Coniglio A, Ghidoni S, Giovanelli M, Benetti A, Tiberio GA, Giulini SM. Early and late recurrence after liver resection for hepatocellular carcinoma: prognostic and therapeutic implications. Ann Surg 2006;243:229-35.
4. Shah SA, Greig PD, Gallinger S, Cattral MS, Dixon E, Kim RD, Taylor BR, Grant DR, Vollmer CM. Factors associated with early recurrence after resection for hepatocellular carcinoma and outcomes. J Am Coll Surg 2006;202:275-83.
5. Lauwers GY, Terris B, Balis UJ, Batts KP, Regimbeau JM, Chang Y, Graeme-Cook F, Yamabe H, Ikai I, Cleary KR, Fujita S, Flejou JF, Zukerberg LR, Nagorney DM, Belghiti J, Yamaoka Y, Vauthey JN. Prognostic histologic indicators of curatively resected hepatocellular carcinomas: a multi-institutional analysis of 425 patients with definition of a histologic prognostic index. Am J Surg Pathol 2002;26:25-34.
6. Ren Z, He S, Fan X, He F, Sang W, Bao Y, Ren W, Zhao J,

Ji X, Wen H. Survival prediction model for postoperative hepatocellular carcinoma patients. Medicine (Baltimore) 2017;96:e7902.
7. Yamashita Y, Tsuijita E, Takeishi K, Fujiwara M, Kira S, Mori M, Aishima S, Taketomi A, Shirabe K, Ishida T, Maehara Y. Predictors for microinvasion of small hepatocellular carcinoma ≤ 2 cm. Ann Surg Oncol 2012;19:2027-34.
8. Zhou L, Rui JA, Wang SB, Chen SG, Qu Q. Clinicopathological predictors of poor survival and recurrence after curative resection in hepatocellular carcinoma without portal vein tumor thrombosis. Pathol Oncol Res 2015;21:131-8.
9. Zhou L, Rui JA, Zhou WX, Wang SB, Chen SG, Qu Q. Edmondson-Steiner grade: a crucial predictor of recurrence and survival in hepatocellular carcinoma without microvascular invasion. Pathol Res Pract 2017;213:824-30.
10. Yuan Z, Zhang J, Yang H, Ye XD, Xu LC, Li WT. Diffusion-Weighted MR Imaging of Hepatocellular Carcinoma: Current Value in Clinical Evaluation of Tumor Response to Locoregional Treatment. J Vasc Interv Radiol 2016;27:20-30.
11. Wu LM, Xu JR, Lu Q, Hua J, Chen J, Hu J. A pooled analysis of diffusion-weighted imaging in the diagnosis of hepatocellular carcinoma in chronic liver diseases. J Gastroenterol Hepatol 2013;28:227-34.
12. Saito K, Tajima Y, Harada TL. Diffusion-weighted imaging of the liver: Current applications. World J Radiol 2016;8:857-67.
13. Nakanishi M, Chuma M, Hige S, Omatsu T, Yokoo H, Nakanishi K, Kamiyama T, Kubota K, Haga H, Matsuno Y, Onodera Y, Kato M, Asaka M. Relationship between diffusion-weighted magnetic resonance imaging and histological tumor grading of hepatocellular carcinoma. Ann Surg Oncol 2012;19:1302-9.
14. Chilla GS, Tan CH, Xu C, Poh CL. Diffusion weighted magnetic resonance imaging and its recent trend-a survey. Quant Imaging Med Surg 2015;5:407-22.
15. Le Bihan D. Molecular diffusion nuclear magnetic resonance imaging. Magn Reson Q 1991;7:1-30.
16. Jensen JH, Helpern JA. MRI quantification of non-Gaussian water diffusion by kurtosis analysis. NMR Biomed 2010;23:698-710.
17. Jensen JH, Helpern JA, Ramani A, Lu H, Kaczynski K. Diffusional kurtosis imaging: the quantification of non-gaussian water diffusion by means of magnetic resonance imaging. Magn Reson Med 2005;53:1432-40.
18. Rosenkrantz AB, Padhani AR, Chenevert TL, Koh DM, De Keyzer F, Taouli B, Le BD. Body diffusion kurtosis imaging: Basic principles, applications, and considerations for clinical practice. J Magn Reson Imaging 2015;42:1190-202.
19. Jambor I, Merisaari H, Taimen P, Boström P, Minn H, Pesola M, Aronen HJ. Evaluation of different mathematical models for diffusion-weighted imaging of normal prostate and prostate cancer using high b-values: a repeatability study. Magn Reson Med 2015;73:1988-98.
20. Chen T, Li Y, Lu SS, Zhang YD, Wang XN, Luo CY, Shi HB. Quantitative evaluation of diffusion-kurtosis imaging for grading endometrial carcinoma: a comparative study with diffusion-weighted imaging. Clin Radiol 2017;72:995.e11-20.
21. Sun K, Chen X, Chai W, Fei X, Fu C, Yan X, Zhan Y, Chen K, Shen K, Yan F. Breast Cancer: Diffusion Kurtosis MR Imaging Diagnostic Accuracy and Correlation with Clinical-Pathologic Factors. Radiology 2015;277:46-55.
22. Rosenkrantz AB, Sigmund EE, Johnson G, Babb JS, Mussi TC, Melamed J, Taneja SS, Lee VS, Jensen JH. Prostate cancer: feasibility and preliminary experience of a diffusional kurtosis model for detection and assessment of aggressiveness of peripheral zone cancer. Radiology 2012;264:126-35.
23. Payabvash S. Quantitative diffusion magnetic resonance imaging in head and neck tumors. Quant Imaging Med Surg 2018;8:1052-65.
24. Rosenkrantz AB, Sigmund EE, Winnick A, Niver BE, Spieler B, Morgan GR, Hajdu CH. Assessment of hepatocellular carcinoma using apparent diffusion coefficient and diffusion kurtosis indices: preliminary experience in fresh liver explants. Magn Reson Imaging 2012;30:1534-40.
25. Wang WT, Yang L, Yang ZX, Hu XX, Ding Y, Yan X, Fu CX, Grimm R, Zeng MS, Rao SX. Assessment of Microvascular Invasion of Hepatocellular Carcinoma with Diffusion Kurtosis Imaging. Radiology 2018;286:571-80.
26. Roayaie S, Blume IN, Thung SN, Guido M, Fiel MI, Hiotis S, Labow DM, Llovet JM, Schwartz ME. A system of classifying microvascular invasion to predict outcome after resection in patients with hepatocellular carcinoma. Gastroenterology 2009;137:850-5.
27. Edmondson HA, Steiner PE. Primary carcinoma of the liver: a study of 100 cases among 48,900 necropsies. Cancer 1954;7:462-503.
28. Goshima S, Kanematsu M, Noda Y, Kondo H, Watanabe H, Bae KT. Diffusion kurtosis imaging to assess response to treatment in hypervascular hepatocellular carcinoma. AJR Am J Roentgenol 2015;204:W543-9.
29. Okamura S, Sumie S, Tonan T, Nakano M, Satani M, Shimose S, Shirono T, Iwamoto H, Aino H, Niizeki T,

Tajiri N, Kuromatsu R, Okuda K, Nakashima O, Torimura T. Diffusion-weighted magnetic resonance imaging predicts malignant potential in small hepatocellular carcinoma. Dig Liver Dis 2016;48:945-52.
30. Jiang T, Xu JH, Zou Y, Chen R, Peng LR, Zhou ZD, Yang M. Diffusion-weighted imaging (DWI) of hepatocellular carcinomas: a retrospective analysis of the correlation between qualitative and quantitative DWI and tumour grade. Clin Radiol 2017;72:465-72.
31. Chen J, Wu M, Liu R, Li S, Gao R, Song B. Preoperative evaluation of the histological grade of hepatocellular carcinoma with diffusion-weighted imaging: a meta-analysis. PLoS One 2015;10:e0117661.
32. Xu P, Zeng M, Liu K, Shan Y, Xu C, Lin J. Microvascular invasion in small hepatocellular carcinoma: is it predictable with preoperative diffusion-weighted imaging. J Gastroenterol Hepatol 2014;29:330-6.
33. Suh YJ, Kim MJ, Choi JY, Park MS, Kim KW. Preoperative Prediction of the Microvascular Invasion of Hepatocellular Carcinoma with Diffusion-Weighted Imaging. Liver Transpl 2012;18:1171-8.
34. Zhao J, Li X, Zhang K, Yin X, Meng X, Han L, Zhang X. Prediction of microvascular invasion of hepatocellular carcinoma with preoperative diffusion-weighted imaging A comparison of mean and minimum apparent diffusion coefficient values. Medicine (Baltimore) 2017;96:e7754.
35. Li H, Zhang J, Zheng Z, Guo Y, Chen M, Xie C, Zhang Z, Mei Y, Feng Y, Xu Y. Preoperative histogram analysis of intravoxel incoherent motion (IVIM) for predicting microvascular invasion in patients with single hepatocellular carcinoma. Eur J Radiol 2018;105:65-71.
36. Budjan J, Sauter EA, Zoellner FG, Lemke A, Wambsganss J, Schoenberg SO, Attenberger UI. Diffusion kurtosis imaging of the liver at 3 Tesla: in vivo comparison to standard diffusion-weighted imaging. Acta Radiol 2018;59:18-25.
37. Iima M, Le BD. Clinical Intravoxel Incoherent Motion and Diffusion MR Imaging: Past, Present, and Future. Radiology 2016;278:13-32.
38. Zhou Y, He L, Huang Y, Chen S, Wu P, Ye W, Liu Z, Liang C. CT-based radiomics signature: a potential biomarker for preoperative prediction of early recurrence in hepatocellular carcinoma. Abdom Radiol (NY) 2017;42:1695-704.
39. Yang T, Lin C, Zhai J, Shi S, Zhu M, Zhu N, Lu JH, Yang GS, Wu MC. Surgical resection for advanced hepatocellular carcinoma according to Barcelona Clinic Liver Cancer (BCLC) staging. J Cancer Res Clin Oncol 2012;138:1121-9.
40. An C, Kim DW, Park YN, Chung YE, Rhee H, Kim MJ. Single Hepatocellular Carcinoma: Preoperative MR Imaging to Predict Early Recurrence after Curative Resection. Radiology 2015;276:433-43.
41. Lee S, Kim SH, Hwang JA, Lee JE, Ha SY Pre-operative ADC predicts early recurrence of HCC after curative resection. Eur Radiol 2019;29:1003-12.
42. Hu F, Tang W, Sun Y, Wan D, Cai S, Zhang Z, Grimm R, Yan X, Fu C, Tong T, Peng W. The value of diffusion kurtosis imaging in assessing pathological complete response to neoadjuvant chemoradiation therapy in rectal cancer: a comparison with conventional diffusion-weighted imaging. Oncotarget 2017;8:75597-606.
43. Cui Y, Yang X, Du X, Zhuo Z, Xin L, Cheng X Whole-tumour diffusion kurtosis MR imaging histogram analysis of rectal adenocarcinoma: Correlation with clinical pathologic prognostic factors. Eur Radiol 2018;28:1485-94.
44. Merisaari H, Jambor I. Optimization of b-value distribution for four mathematical models of prostate cancer diffusion-weighted imaging using b values up to 2000 s/mm(2): simulation and repeatability study. Magn Reson Med 2015;73:1954-69.
45. Chen X, Qin L, Pan D, Huang Y, Yan L, Wang G, Liu Y, Liang C, Liu Z. Liver diffusion-weighted MR imaging: reproducibility comparison of ADC measurements obtained with multiple breath-hold, free-breathing, respiratory-triggered, and navigator-triggered techniques. Radiology 2014;271:113-25.
46. Shan Y, Zeng MS, Liu K, Miao XY, Lin J, Cx F, Xu PJ. Comparison of Free-Breathing with Navigator-Triggered Technique in Diffusion Weighted Imaging for Evaluation of Small Hepatocellular Carcinoma: Effect on Image Quality and Intravoxel Incoherent Motion Parameters. J Comput Assist Tomogr 2015;39:709-15.

Cite this article as: Cao L, Chen J, Duan T, Wang M, Jiang H, Wei Y, Xia C, Zhou X, Yan X, Song B. Diffusion kurtosis imaging (DKI) of hepatocellular carcinoma: correlation with microvascular invasion and histologic grade. Quant Imaging Med Surg 2019;9(4):590-602. doi: 10.21037/qims.2019.02.14

